

Superinjection in Diamond P-I-N Diodes: Bright Single-Photon Electroluminescence of Color Centers Beyond the Doping Limit

Igor A. Khramtsov, and Dmitry Yu. Fedyanin*

Laboratory of Nanooptics and Plasmonics, Moscow Institute of Physics and Technology, 141700

Dolgoprudny, Russian Federation

*email: dmitry.fedyanin@phystech.edu

ABSTRACT

Efficient generation of single photons on demand at a high repetition rate is a key to the practical realization of quantum-communication networks and optical quantum computations. Color centers in diamond are considered to be the most promising platform for building such single-photon sources owing to the outstanding emission properties of color centers at room temperature. However, their efficient electrical excitation remains a challenge due to the inability to create a high density of free electrons in diamond. Here, we demonstrate that using the self-gating effect in a diamond p-i-n diode, one can overcome the doping problem and inject four orders of magnitude more carriers into the i-region of the diamond diode than the doping of the n-region allows. This high density of free electrons can be efficiently used to boost the single-photon electroluminescence process and enhance the brightness of the single-photon source by more than three orders of magnitude. Moreover, we show that such a high single-photon emission rate can be achieved at exceptionally low injection current densities of only 0.001 A/mm^2 , which creates the backbone for the development of low-power and cost-efficient diamond quantum optoelectronic devices for quantum information technologies.

I. INTRODUCTION

Single color centers in diamond are currently considered as one of the most promising platforms for building a practical single-photon source – the device which is a key element for most applications of quantum information science [1–3]. One of the most important advantages of diamond over other platforms, such as quantum dots [4] and point defects in different 3D, 2D and 1D semiconductors [5–10], is an exceptionally weak electron-phonon interaction [11]. Diamond features a record Debye temperature of 2200 K [12]. Therefore, the emission spectra of many point defects in the crystal lattice of diamond (such as the silicon-vacancy (SiV) [13–15] and germanium-vacancy (GeV) centers [13,16]) exhibit a remarkably sharp peak with a dim phonon-sideband emission even at room temperature [13]. For example, more than 75% of photons emitted by the SiV center go into the zero-phonon line (ZPL) [14,15], while the spectral width of the ZPL is less than 1 nm [14]. These defects can be created with high positioning accuracy (30 – 50 nm [17]) at any point of the nanostructure using the focused ion beam implantation. In addition, due to the large bandgap, diamond is transparent in the visible and in infrared, while the indirect nature of the bandgap ensures a very low background luminescence level under both optical and electrical excitations. Such remarkable properties of color centers in diamond can hardly be achieved with other solid-state quantum systems at ambient conditions [5–10].

The outstanding optical properties combined with the possibility to trigger color centers electrically on demand [18–23] are exactly what is required for building practical quantum information devices which operate at room temperature. However, it is not easy to efficiently excite color centers in diamond electrically by embedding them in a p-n or p-i-n diode [18–22].

Diamond is a material at the interface between semiconductors and insulators. This means that

the conductivity of diamond cannot be as high as that of conventional semiconductors, such as silicon or gallium arsenide. The problem is especially pronounced in n-type samples since the activation energy of donors in diamond (~ 0.6 eV [24]) is an order of magnitude higher than in silicon ($0.03 - 0.07$ eV [25]). This high activation energy along with the unavoidable acceptor-type defects, which compensate donors in n-type samples, reduce the maximum density of free electrons at room temperature to $\sim 10^{10}$ cm $^{-3}$ [24,26] [see Fig. 1(a)]. This is much lower than what can be created in most semiconductor materials. In turn, the photon emission rate by color centers is determined by the carrier capture processes [27,28]. It is proportional to the densities of free electrons and holes in the vicinity of the color center. Therefore, due to the high activation energy of donors in diamond, the maximum photon emission rate is limited approximately by $\Phi \times \min(c_p p_{\text{eqp}}, c_n n_{\text{eqn}})$, where n_{eqn} is the density of free electrons in the n-type region of the diamond structure in equilibrium, p_{eqp} is the density of holes in the p-type region in equilibrium, Φ is the quantum efficiency of the color center, c_n and c_p are the capture rate constants, which characterize the processes of the electron and hole capture by the color center (for details, see Refs 27,28). Simple estimations show that at room temperature, the photon emission rate should not exceed ~ 1 kcps for most diamond samples [Fig. 1(b)]. Taking into account that typically only a few percent of photons can be collected by an optical objective [2], the observed photon count rate is nearly two orders of magnitude lower, which is not enough for practical applications. At high temperatures, electrically pumped color centers can be significantly brighter [27], but the emission properties of color centers are inferior to those at room temperature and are less suited for quantum optics applications.

Here, we demonstrate that using the self-gating effect in a diamond p-i-n diode, even at room temperature, the single-photon electroluminescence (SPEL) rate of color centers embedded in a

p-i-n diode can be increased to about 1 Mcps, which is three orders of magnitude above the doping limit. Moreover, we show that this rate can be achieved at current densities as low as 0.001 A/mm^2 , which is particularly favorable for practical applications.

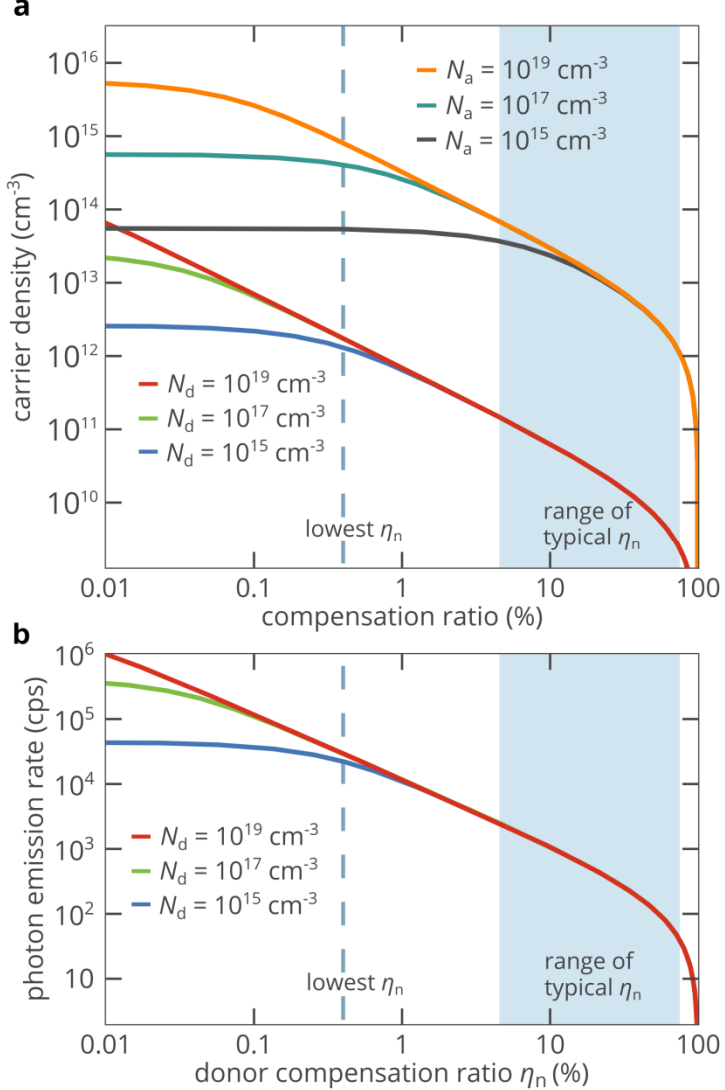


FIG. 1. (a) Free electron density in n-type diamond versus donor compensation ratio η_n . Also plotted is the dependence of the density of holes in p-type diamond as a function of the acceptor compensation ratio η_p . The blue-shaded area shows the range of donor compensation ratios which are typical for n-type diamond samples, while the blue dashed vertical line indicates the lowest reported, to the best of our knowledge, donor compensation ratio of $\eta_n = 0.4\%$ [29]. (b)

Estimated maximum photon emission rate of the color center as a function of the donor compensation ratio. The density of holes in the vicinity of the color center is assumed to be equal to $3.2 \times 10^{14} \text{ cm}^{-3}$ and the quantum efficiency is set to 100%.

II. RESULTS AND DISCUSSION

Fig. 2(a) shows a schematic illustration of the single-photon emitting diamond p-i-n diode. The color center is incorporated in the i-region of the diode to reduce its interaction with impurities and defects in the n-type and p-type regions. Due to the high activation energies of donors and acceptors, such a diamond diode cannot be described analytically, especially at high forward bias voltages. Therefore, we performed self-consistent numerical simulations of the electron and hole transport based on the Poisson equation, drift-diffusion current equations, and the electron and hole continuity equations using the nextnano++ software [30]. The p-region is doped with boron at a concentration of 10^{18} cm^{-3} . The boron acceptors are partially compensated by donor-type defects, the compensation ratio is $\eta_p = 1\%$ [31], which corresponds to the density of holes of $3.2 \times 10^{14} \text{ cm}^{-3}$ [Fig. 1(a)]. The concentration of phosphorus donors in the n-region is also equal to 10^{18} cm^{-3} , but the donor compensation ratio is significantly higher and equals $\eta_n = 10\%$, which is typical for n-type diamond samples [24,26,32]. For other parameters used in the simulations, see Table S1 in Supplemental Material [33]. In equilibrium, the maximum density of electrons in the p-i-n diode is found in the n-region and equals $n_{\text{eqn}} = 6.3 \times 10^{10} \text{ cm}^{-3}$ [Fig. 1(a)], which virtually limits the photon emission rate of the color center to about $c_n n_{\text{eqn}} = 1000 \text{ s}^{-1}$ at low and moderate injection currents. However, our simulations show that at high injection levels, i.e. at high forward bias voltages, the situation is significantly different.

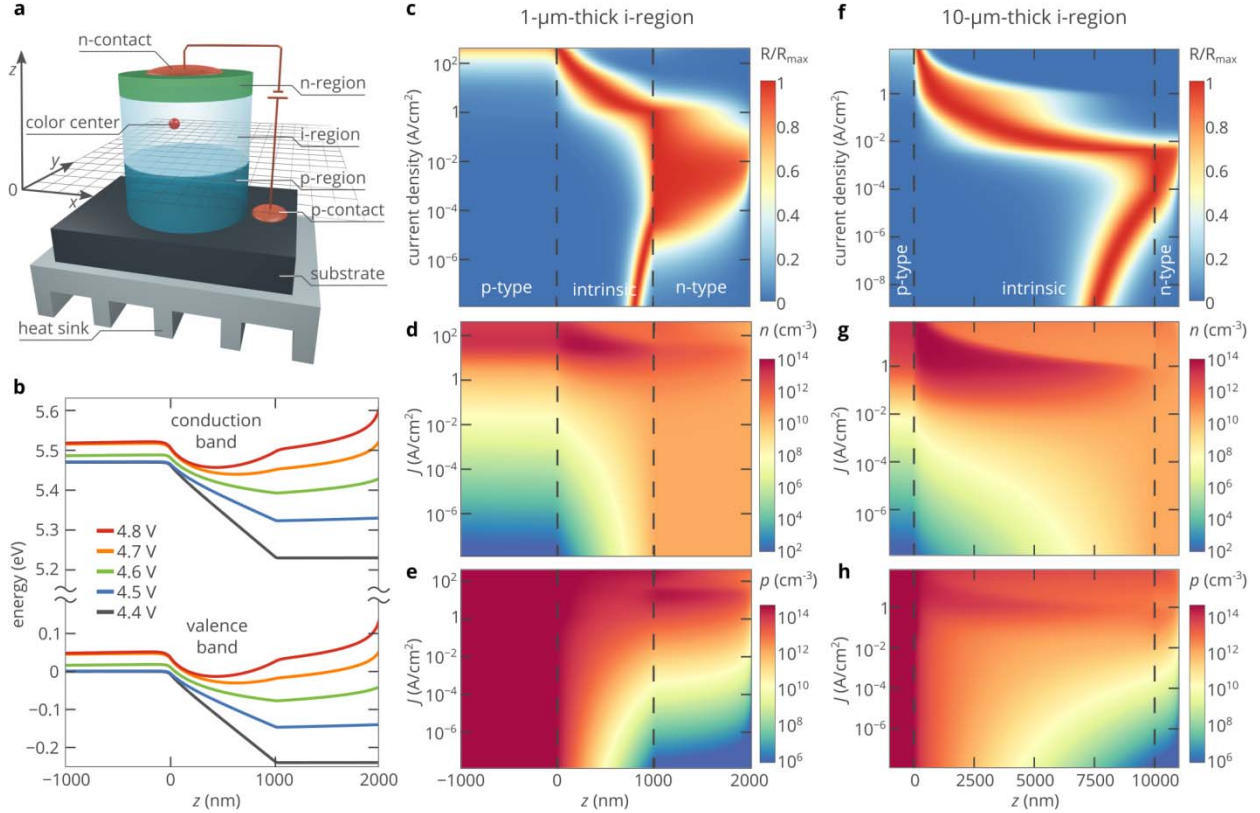


FIG. 2. (a) Schematic illustration of the single-photon emitting diamond p-i-n diode. The substrate is mounted to a heat sink to maintain the diode temperature at about 300 K. (b) Energy band diagram for the p-i-n diode with a 1-μm-thick i-region. (c) Distribution of the normalized SPEL rate as a function of the pump current. The SPEL rate is normalized to the maximum achievable SPEL rate at the same pump current. (d,e) Evolution of the electron (d) and hole (e) distributions in the p-i-n diode with the pump current. In panels c-e, the thickness of the i-region of the p-i-n diode is equal to 1 μm. (f-h) Spatial distributions of normalized SPEL rate (f), electron density (g) and hole density (h) as a function of the pump current. In panels f-h, the thickness of the i-region is equal to 10 μm.

Figure 2(c) shows the obtained normalized photon emission rate of the color center as a function of the injection current and the position of the color center in the p-i-n diode with a 1- μm -thick intrinsic region. It is important to note here that Fig. 2 and most other figures discussed below are valid for most color centers in diamond which have two charge states: negatively charged and neutral. The reason for this is that the process of color-center electroluminescence is essentially based on the electron and hole exchange between the color center and the diamond crystal. This implies the processes of free-carrier capture (both electrons and holes) and free-exciton capture [27,28,34]. At room and higher temperatures, the contribution of the latter process is usually significantly weaker than that of the former (for details, see Ref. [28]). The hole capture cross-section by the negatively charged color center is mostly determined by the properties of diamond rather than by the internal structure of the defect [27], while the electron capture cross-section by the color center in the neutral charge state is roughly equal to the lattice constant of diamond and can only slightly vary from one defect to another [35–37], which is due to the different structure of the defects. Returning to Fig. 2c, one can easily distinguish three injection regimes: the first is at current densities below 10^{-5} A/cm^2 , the second is in the range from 10^{-5} to 1 A/cm^2 , and the third regime corresponds to higher currents.

To understand the interesting evolution of the distribution of the photon emission rate with the injection current shown in Fig. 2c, we move on to the equation for the photon emission rate [27].

$$R = \Phi \frac{1}{(c_n n)^{-1} + (c_p p)^{-1} + \Phi \tau_r} \quad (1)$$

Here, τ_r is the radiative lifetime of the excited state, Φ is the quantum efficiency and n and p are the densities of electrons and holes in the vicinity of the color center. Both SiV and GeV centers have two charge states: neutral and negatively charged [16,19]. Therefore, as discussed above,

the capture rate constants are roughly the same for both centers and equal $c_n = 1.7 \times 10^{-8} \text{ cm}^3 \text{s}^{-1}$ and $c_p = 3.9 \times 10^{-7} \text{ cm}^3 \text{s}^{-1}$ at room temperature [27]. Equation (1) shows that since the lifetime of the excited state for both SiV and GeV centers is in the nanosecond range [14,16], the SPEL rate R is determined only by relatively slow electron and hole capture processes as shown below.

Fig. 2(d,e) presents the simulated distributions of electrons and holes at different injection currents. In equilibrium, there are no free carriers in the i-region of the diode. As the bias increases, electrons are injected from the n-region and holes are injected from the p-region. Since p_{eqp} is much higher than n_{eqn} , in the i-region, the density of holes is also higher than the density of electrons everywhere except the area near the i-n junction. Taking into account that the $c_p > c_n$, we obtain that at low injection levels, the optimum position of the color center, i.e. the position where the highest emission rate can be achieved, is in the very proximity of the i-n junction. As the current increases, the maximum photon emission rate R_{max} that can be obtained at a fixed injection current also increases (see Fig. 3), and the optimum position of the color center is shifted to the n-region [see Fig. 2(c)], since more and more holes are injected into the i-region and these carriers penetrate deeper into the i-region.

When the density of holes at the i-n junction exceeds $\sim 3c_n n_{\text{eqn}}/c_p = 0.8 \times 10^{10} \text{ cm}^{-3}$, the only limitation on the photon emission rate is the electron capture rate $c_n n_{\text{eqn}}$ (the doping limit) as follows from Eq. (1). Therefore, we observe a plateau in the input-output curve at current densities above 10^{-4} A/cm^2 (Fig. 3). The photon emission rate does not further increase with the pump current. The height of this plateau is mostly determined by the density n_{eqn} of free electrons in the n-type region. The SPEL rate in the n-region is significantly higher than that in the i-region, and the optimum position of the color center appears exactly at the i-n junction [Fig. 2(c)]. In conventional semiconductors, such as silicon or gallium arsenide, we would

observe this plateau even at extremely high bias voltages. However, in the considered diamond p-i-n diode, the photon emission rate suddenly leaves the plateau and exceeds the doping limit at a current density of $J = 0.13 \text{ A/cm}^2$ (Fig. 3).

The band diagram shown in [Fig. 2(b)] explains the unexpected rapid increase in the SPEL rate. At a bias voltage of $V = 4.5 \text{ V}$ (which corresponds to $J = 0.035 \text{ A/cm}^2$), a hardly recognizable potential well for electrons is formed in the i-region in the vicinity of the i-n junction. Free electrons are accumulated in this potential well. The potential well for electrons is at the same time a potential barrier for holes. As the bias increases, the depth of the potential well increases and its bottom is shifted towards the p-region of the diode [Fig. 2(b)], which is clearly seen at biases of 4.7 and 4.8 V. The optimum position for the color center coincides with the bottom of the potential well, which is also shifted towards the p-region. Eventually, at very high bias voltages, the well is found in the very vicinity of the p-i junction.

The observed effect is similar to the effect of the gate electrode in a field effect transistor and could be referred as the self-gating effect. This is more an inverse self-gating effect rather than the direct one. In [Fig. 2(b)], one can see a flat-band p-region, while the band bending is strong in the i- and n-regions. The region of the potential well for electrons (potential barrier for holes) is a bridge between two regions with different types of conductivity (diffusion conductivity in the p-region and drift conductivity in the i- and n-regions). Due to the high asymmetry of the p-i-n structure, i.e. due to the huge difference in electrical properties of the n-type and p-type regions, the potential well is significantly deep at moderate and high bias voltages. This gives the possibility to accumulate a very high density of free electrons in the well, namely one can inject nearly four orders of magnitude more electrons than the doping of the n-type region allows [Fig. 2(d)]. It is interesting that in this high-injection regime, the density of electrons in the well

increases rapidly with the injection current and the slope dR_{\max}/dJ appears higher than at low injection levels (see the blue curve in Fig. 3). However, at $J = 42 \text{ A/cm}^2$, R_{\max} reaches its maximum and then decreases. This roll-over looks very similar to that of semiconductor lasers [38], but the physical origin is entirely different. At a very high injection current, due to the relatively low resistivity of diamond, the bias voltage is very high and a strong linear band bending is observed in both the n-type and p-type regions, which is very different from the well-known flat-band condition in conventional semiconductor diodes at very high injection levels [39]. In this case, the drift transport dominates over the diffusion one, and the potential well in the i-region almost completely vanishes, which prevents electrons from accumulating in the i-region and eventually reduces the SPEL rate governed by the electron density (Fig. 3). Therefore, the photon emission rate exhibits a maximum at $J = 42 \text{ A/cm}^2$ ($V = 6.05 \text{ V}$).

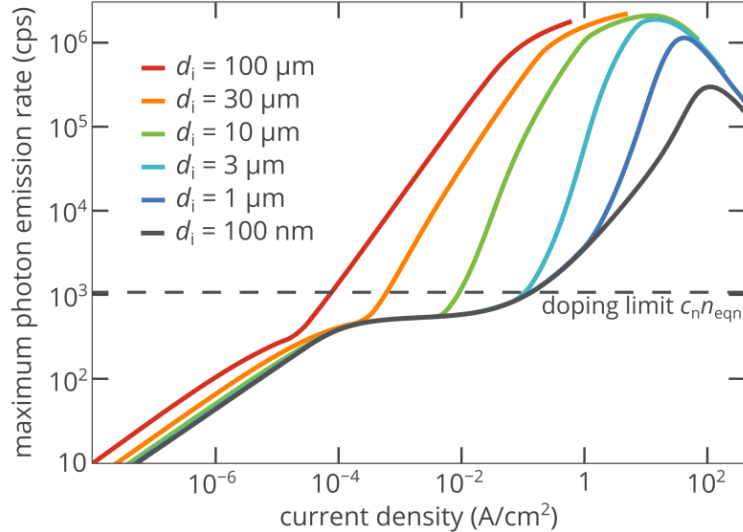


FIG. 3. Maximum photon emission rate R_{\max} that can be obtained from the color center in the p-i-n diode versus injection current for different thicknesses of the intrinsic region of the p-i-n diode. The quantum efficiency is assumed to be equal to 100%.

The strength of the self-gating effect greatly depends on the thickness d_i of the intrinsic region of the p-i-n diode. For small thicknesses, such as $d_i = 100$ nm, the maximum rate is 5 times lower than at $d_i = 1000$ nm. Moreover, the maximum is achieved at a current density as high as 110 A/cm 2 (Fig. 3), which is not favorable for practical applications. On the contrary, as the thickness of the i-region increases, the depth of the potential well in the i-region increases. Accordingly, R_{\max} increases by 50% at $d_i = 10$ μm and is even higher at $d_i = 100$ μm (Fig. 3). More importantly, it is easier to achieve bright single-photon electroluminescence at large thicknesses d_i . For example, a current density of 29 A/cm 2 is needed to reach the photon emission rate of 1 Mcps at $d_i = 1$ μm . At $d_i = 10$ μm and 100 μm , this current reduces to 0.9 A/cm 2 and 0.11 A/cm 2 , respectively. Despite that achieving a high emission rate at larger d_i requires a higher bias voltage, the net power JV supplied to the single-photon source appears to be lower, which is beneficial for practical applications. Our simulations show that at a photon emission rate of 1 Mcps, the single-photon emitting diode with a 100 - μm -thick i-region consumes 200 times less power than the diode with a 1 - μm -thick i-region (see Fig. S1 in Supplemental Material [33]). However, a very thick i-region acts as a series resistance, which leads to bias voltages greater than 10 V. Therefore, from a practical viewpoint, moderate thicknesses ~ 10 – 30 μm are probably more reasonable.

For achieving bright single-photon emission, it is extremely important to place the color center (using, for example, ion implantation) at the optimal position in the i-region of the p-i-n diode, since the position of the color center, which is a point defect in the crystal lattice, is fixed and cannot be tuned during diode exploitation. Figure 4(a) shows the simulated SPEL rate of the color center at five different positions inside i-region of the p-i-n diode with a 10 - μm -thick intrinsic region. At low currents, the brightness is the highest for the color center near the i-n

junction at $z = 9 \mu\text{m}$, which agrees with Fig. 2(f). At $J \approx 0.01 \text{ A/cm}^2$, the optimum position for the color center is shifted towards the p-region, but the rate at $z = 9 \mu\text{m}$ still increases. At $J = 0.5 \text{ A/cm}^2$, the brightest point appears in the vicinity of the p-i junction at $z \approx 1 \mu\text{m}$, and the rate at $z = 9 \mu\text{m}$ begins to decrease towards the doping limit $c_n n_{\text{eqn}}$, since the width of the potential well in the i-region rapidly decreases with the current at $J \gtrsim 0.1 \text{ A/cm}^2$ and the color center at $z = 9 \mu\text{m}$ appears outside the potential well for electrons. A similar trend is observed for the color center at $z = 5 \mu\text{m}$ but at slightly higher currents. In the vicinity of the p-i junction, the SPEL rate of the color center also decreases after reaching a maximum, but the width and the height of the peak are much large and the decrease is related to the disappearance of the potential well at very high bias voltages. The maximum rate at $z = 0.5 \mu\text{m}$ is 5 times higher than in the center of the i-region and 220 times higher than near the i-n junction [Fig. 4(a)]. Our analysis shows that the optimum position for the color center is at a distance of about 200–500 nm from the p-i junction. In this regard, we hold that since the thickness of the i-region should be higher than $10 \mu\text{m}$, it is not reasonable to utilize vertical p-i-n structures [Fig. 2(a)], which were used in recent experimental works [19,22]. It is easier to work with color centers near the diamond surface rather than with color centers placed at depth of 10–100 μm . Therefore, we suggest to fabricate ‘flipped’ structures, i.e. vertical n-i-p diode structures.

Finally, we want to draw attention to the fact that the brightness of the color center at different positions does not necessarily correlate with the characteristic time of the second-order autocorrelation function $g^{(2)}$, e.g., with the half-rise time $\tau_{1/2}$ defined as $g^{(2)}(\tau_{1/2}) = 1/2$. The reason for this is that the characteristic time $\tau_{1/2}$ is determined by the sum $(c_n n + c_p p)$ of the capture rates [28,34] and is, in fact, governed by the fastest process (usually, by the hole capture). At the same time, the SPEL rate is determined by the slowest process (typically, by the electron capture).

This difference is especially pronounced for color centers near the p-i junction, where the density of holes is always higher than the density of electrons (see Fig. 2). In this region, the dynamics of single-photon emission is always faster than that in the center of the i-region or in the vicinity of the i-n junction regardless the injection level [Fig. 4(b-e)]. Moreover, we note that at every point of the i-region of the p-i-n diode, $c_p p / c_n n > 20$ for current densities above 10^{-4} A/cm². Therefore, the widely used $g^{(2)}$ function does not directly or indirectly show the photon rate of the single-photon emitting diode. However, the $g^{(2)}$ function can be efficiently used to measure the density of holes at the position of the color center and monitor the hole injection level.

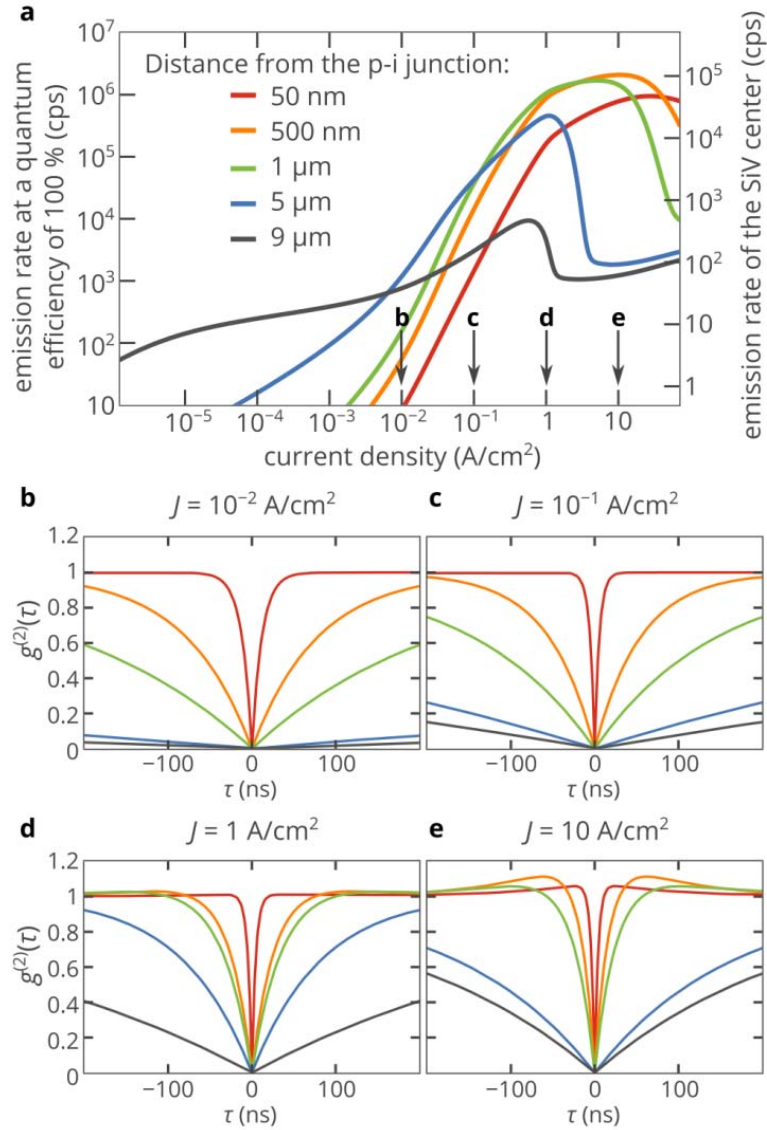


FIG. 4. (a) SPEL rate of the color center with two charge states (negative and neutral) and 100% quantum efficiency and SPEL rate of the SiV center (5% quantum efficiency) versus pump current simulated for five different positions of the color center in the p-i-n diode with a 10-um-thick i-region. (b-e) Simulated $g^{(2)}$ functions of the SiV center at four different injection currents. The notations are the same as in panel a. The lifetime of the excited state equals 1.2 ns and the lifetime of the shelving state is 100 ns [40].

III. CONCLUSIONS

In summary, we have numerically demonstrated the ‘superinjection’ effect in diamond p-i-n diodes. This effect gives the possibility to accumulate a high density of electrons, which is nearly four orders of magnitude above the equilibrium value in the n-type region of the diode, in the i-region in the vicinity of the p-i junction. This effect is not observed in conventional semiconductors, such as silicon or gallium arsenide, due to the low resistivity of the n- and p-type regions of the diode structure. In diamond, due to the exceptionally high activation energy of donors, the density of free electrons in the n-type region is 6 – 9 orders of magnitude lower than in most semiconductor devices. In addition, the density of holes in the p-type region is roughly 3 – 5 orders of magnitude higher than in the n-region. The high asymmetry between electrical properties of the n- and p-type regions combined with the low densities of carriers provides favorable conditions for the self-gating effect. Under high bias voltages, a potential well for electrons is formed in the i-region at a distance of about 200 – 500 nm from the p-i junction, which is similar to the effect of the gate in a field effect transistor. Electrons are accumulated in this potential well, which is beneficial for exploiting different ‘local’ effects, e.g., for the developing single-photon emitting diodes based on color centers – point defects in the crystal lattice of diamond. Electroluminescence of the color center is based on the electron and hole capture processes. Since the SPEL rate is roughly proportional to the density of electrons in the vicinity of the color center, the superinjection effect can enhance the brightness of the electrically-driven sources by more than three orders of magnitude and reduce the power needed to drive the single-photon source, which is crucial for practical applications. Since it is extremely difficult to create a high density of free electrons in diamond at room temperature, the

demonstrated effect can be used for the design of low-cost but efficient and bright single-photon devices for quantum information and quantum optics applications.

ACKNOWLEDGEMENTS

The work is supported by the Russian Science Foundation (17-79-20421).

REFERENCES

- [1] S. Prawer and I. Aharonovich, *Quantum Information Processing with Diamond: Principles and Applications* (Woodhead Publishing, Cambridge, 2014).
- [2] I. Aharonovich, S. Castelletto, D. A. Simpson, C.-H. Su, A. D. Greentree, and S. Prawer, Diamond-based single-photon emitters, [Rep. Prog. Phys. 74, 076501 \(2011\)](#).
- [3] M. Leifgen, T. Schröder, F. Gädke, R. Riemann, V. Métillon, E. Neu, C. Hepp, C. Arend, C. Becher, K. Lauritsen, and O. Benson, Evaluation of nitrogen- and silicon-vacancy defect centres as single photon sources in quantum key distribution, [New J. Phys. 16, 023021 \(2014\)](#).
- [4] P. Michler, *Single Semiconductor Quantum Dots* (Springer, Berlin, Heidelberg, 2009).
- [5] I. Aharonovich, D. Englund, and M. Toth, Solid-state single-photon emitters, [Nat. Photonics 10, 631 \(2016\)](#).
- [6] S. Choi, A. M. Berhane, A. Gentle, C. Ton-That, M. R. Phillips, and I. Aharonovich, Electroluminescence from Localized Defects in Zinc Oxide: Toward Electrically Driven Single Photon Sources at Room Temperature, [ACS Appl. Mater. Interfaces 7, 5619 \(2015\)](#).
- [7] T. T. Tran, M. Kianinia, M. Nguyen, S. Kim, Z.-Q. Xu, A. Kubanek, M. Toth, and I. Aharonovich, Resonant Excitation of Quantum Emitters in Hexagonal Boron Nitride, [ACS Photonics \(to be published\)](#).

[8] A. M. Berhane, C. Bradac, and I. Aharonovich, Photoinduced blinking in a solid-state quantum system, [Phys. Rev. B **96**, 041203 \(2017\)](#).

[9] C. Palacios-Berraquero, D. M. Kara, A. R.-P. Montblanch, M. Barbone, P. Latawiec, D. Yoon, A. K. Ott, M. Loncar, A. C. Ferrari, and M. Atatüre, Large-scale quantum-emitter arrays in atomically thin semiconductors, [Nat. Commun. **8**, 15093 \(2017\)](#).

[10] X. He, N. F. Hartmann, X. Ma, Y. Kim, R. Ihly, J. L. Blackburn, W. Gao, J. Kono, Y. Yomogida, A. Hirano, T. Tanaka, H. Kataura, H. Htoon, and S. K. Doorn, Tunable room-temperature single-photon emission at telecom wavelengths from sp3 defects in carbon nanotubes, [Nat. Photonics **11**, 577 \(2017\)](#).

[11] L. S. Pan and D. R. Kania, *Diamond: Electronic Properties and Applications* (Springer, Berlin, 1995).

[12] Authors and Editors of the LB Volumes III/17A-22A-41A1b, Diamond (C), Debye temperature, heat capacity, density, hardness, melting point and related data, in *Group IV Elements, IV-IV and III-V Compounds. Part B - Electronic, Transport, Optical and Other Properties*, edited by O. Madelung, U. Rössler, and M. Schulz (Springer, Berlin, 2002).

[13] S. Häußler, G. Thiering, A. Dietrich, N. Waasem, T. Teraji, J. Isoya, T. Iwasaki, M. Hatano, F. Jelezko, A. Gali, and A. Kubanek, Photoluminescence excitation spectroscopy of SiV- and GeV- color center in diamond, [New J. Phys. **19**, 063036 \(2017\)](#).

[14] E. Neu, D. Steinmetz, J. Riedrich-Möller, S. Gsell, M. Fischer, M. Schreck, and C. Becher, Single photon emission from silicon-vacancy colour centres in chemical vapour deposition nano-diamonds on iridium, [New J. Phys. **13**, 025012 \(2011\)](#).

[15] S. Lagomarsino, F. Gorelli, M. Santoro, N. Fabbri, A. Hajeb, S. Sciortino, L. Palla, C. Czelusniak, M. Massi, F. Taccetti, L. Giuntini, N. Gelli, D. Y. Fedyanin, F. S. Cataliotti, C.

Toninelli, and M. Agio, Robust luminescence of the silicon-vacancy center in diamond at high temperatures, [AIP Adv. 5, 127117 \(2015\)](#).

[16] T. Iwasaki, F. Ishibashi, Y. Miyamoto, Y. Doi, S. Kobayashi, T. Miyazaki, K. Tahara, K. D. Jahnke, L. J. Rogers, B. Naydenov, F. Jelezko, S. Yamasaki, S. Nagamachi, T. Inubushi, N. Mizuochi, and M. Hatano, Germanium-Vacancy Single Color Centers in Diamond, [Sci. Rep. 5, 12882 \(2015\)](#).

[17] T. Schröder, M. E. Trusheim, M. Walsh, L. Li, J. Zheng, M. Schukraft, A. Sipahigil, R. E. Evans, D. D. Sukachev, C. T. Nguyen, J. L. Pacheco, R. M. Camacho, E. S. Bielejec, M. D. Lukin, and D. Englund, Scalable focused ion beam creation of nearly lifetime-limited single quantum emitters in diamond nanostructures, [Nat. Commun. 8, 15376 \(2017\)](#).

[18] B. Tegetmeyer, C. Schreyvogel, N. Lang, W. Müller-Sebert, D. Brink, and C. E. Nebel, Electroluminescence from silicon vacancy centers in diamond p–i–n diodes, [Diam. Relat. Mater. 65, 42 \(2016\)](#).

[19] A. M. Berhane, S. Choi, H. Kato, T. Makino, N. Mizuochi, S. Yamasaki, and I. Aharonovich, Electrical excitation of silicon-vacancy centers in single crystal diamond, [Appl. Phys. Lett. 106, 171102 \(2015\)](#).

[20] A. M. Zaitsev, A. A. Bergman, A. A. Gorokhovsky, and M. Huang, Diamond light emitting diode activated with Xe optical centers, [Phys. Status Solidi 203, 638 \(2006\)](#).

[21] A. Lohrmann, S. Pezzagna, I. Dobrinets, P. Spinicelli, V. Jacques, J.-F. Roch, J. Meijer, and A. M. Zaitsev, Diamond based light-emitting diode for visible single-photon emission at room temperature, [Appl. Phys. Lett. 99, 251106 \(2011\)](#).

[22] N. Mizuochi, T. Makino, H. Kato, D. Takeuchi, M. Ogura, H. Okushi, M. Nothaft, P. Neumann, A. Gali, F. Jelezko, J. Wrachtrup, and S. Yamasaki, Electrically driven single-photon

source at room temperature in diamond, [Nat. Photonics 6, 299 \(2012\)](#).

[23] J. Forneris, P. Traina, D. G. Monticone, G. Amato, L. Boarino, G. Brida, I. P. Degiovanni, E. Enrico, E. Moreva, V. Grilj, N. Skukan, M. Jakšić, M. Genovese, and P. Olivero, Electrical stimulation of non-classical photon emission from diamond color centers by means of sub-superficial graphitic electrodes, [Sci. Rep. 5, 15901 \(2015\)](#).

[24] I. Stenger, M.-A. Pinault-Thaury, T. Kociniewski, A. Lusson, E. Chikoidze, F. Jomard, Y. Dumont, J. Chevallier, and J. Barjon, Impurity-to-band activation energy in phosphorus doped diamond, [J. Appl. Phys. 114, 073711 \(2013\)](#).

[25] R. F. Pierret, *Advanced Semiconductor Fundamentals*, 2nd Edition (Pearson Education, New Jersey, 2003).

[26] M. Katagiri, J. Isoya, S. Koizumi, and H. Kanda, Lightly phosphorus-doped homoepitaxial diamond films grown by chemical vapor deposition, [Appl. Phys. Lett. 85, 6365 \(2004\)](#).

[27] D. Yu. Fedyanin and M. Agio, Ultrabright single-photon source on diamond with electrical pumping at room and high temperatures, [New J. Phys. 18, 073012 \(2016\)](#).

[28] I. A. Khramtsov, M. Agio, and D. Y. Fedyanin, Dynamics of Single-Photon Emission from Electrically Pumped Color Centers, [Phys. Rev. Applied 8, 024031 \(2017\)](#).

[29] R. Sauer, N. Teofilov, K. Thonke, and S. Koizumi, Donor-related cathodoluminescence in phosphorus-doped CVD diamond, [Diam. Relat. Mater. 13, 727 \(2004\)](#).

[30] S. Birner, T. Zibold, T. Andlauer, T. Kubis, M. Sabathil, A. Trellakis, and P. Vogl, nextnano: General Purpose 3-D Simulations, [IEEE Trans. Electron Devices 54, 2137 \(2007\)](#).

[31] M. Gabrysch, S. Majdi, A. Hallén, M. Linnarsson, A. Schöner, D. Twitchen, and J. Isberg, Compensation in boron-doped CVD diamond, [Phys. Status Solidi 205, 2190 \(2008\)](#).

[32] I. Stenger, M.-A. Pinault-Thaury, A. Lusson, T. Kociniewski, F. Jomard, J. Chevallier, and J. Barjon, Quantitative analysis of electronic absorption of phosphorus donors in diamond, [Diam. Relat. Mater. 74, 24 \(2017\).](#)

[33] See Supplemental Material at [link] for the photon emission rate dependence on the power and parameters used in the simulations.

[34] I. A. Khramtsov, M. Agio, and D. Y. Fedyanin, Kinetics of single-photon emission from electrically pumped NV centers in diamond, [AIP Conference Proceedings 1874, 040014 \(2017\).](#)

[35] C. E. Nebel, Electronic properties of CVD diamond, [Semicond. Sci. Technol. 18, S1 \(2003\).](#)

[36] C. Claeys and E. Simoen, Basic Radiation Damage Mechanisms in Semiconductor Materials and Devices, in *Radiation Effects in Advanced Semiconductor Materials and Devices. Springer Series in Materials Science* (Springer, Berlin, 2002).

[37] K.-C. Kao, *Dielectric Phenomena in Solids: With Emphasis on Physical Concepts of Electronic Processes* (Elsevier, Amsterdam, 2004).

[38] S. S. Saini, S. H. Cho, and M. Dagenais, Thermal considerations in high power semiconductor lasers and semiconductor optical amplifiers, in [Proc. SPIE 6478, Photonics Packaging, Integration, and Interconnects VII, San Jose, 2007](#) edited by A. M. Earman, and R. T. Chen.

[39] S. M. Sze and K. K. Ng, *Physics of Semiconductor Devices* (Wiley, New Jersey, 2006).

[40] S. Castelletto, I. Aharonovich, C. H. Su, and S. Prawer, Impurities in diamond: a new revival for quantum optics, in [Proc. SPIE 7815, Quantum Communications and Quantum Imaging VIII, San Diego, 2010](#) edited by R. E. Meyers, and Y. Shih, K. S. Deacon.

Supplemental Material for
 Superinjection in Diamond P-I-N Diodes: Bright Single-Photon
 Electroluminescence of Color Centers Beyond the Doping Limit

Igor A. Khramtsov and Dmitry Yu. Fedyanin*

*Laboratory of Nano optics and Plasmonics, Moscow Institute of Physics and Technology, 141700
 Dolgoprudny, Russian Federation*

*email: dmitry.fedyanin@phystech.edu

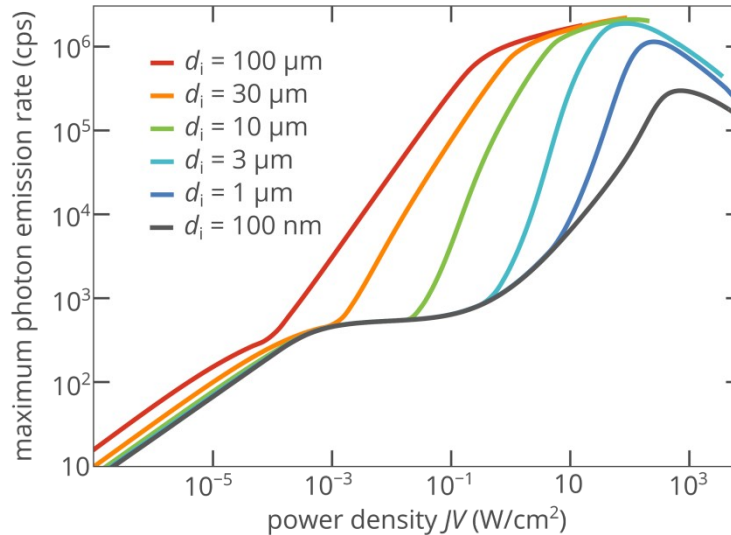


FIG. S1. Maximum photon emission rate R_{\max} that can be obtained from the color center in the p-i-n diode versus pump power density JV for different thicknesses of the intrinsic region of the p-i-n diode. The quantum efficiency is assumed to be equal to 100%.

Table S1. Parameters used in the numerical simulations.

| Parameter | Value | Comment |
|---|---------------------------|-----------|
| Energy band gap of diamond | 5.47 eV | Ref. [S1] |
| Dielectric constant of diamond | 5.7 | Ref. [S1] |
| Density of donors in the n-type region | 10^{18} cm^{-3} | |
| Activation energy of donors | 0.57 eV | Ref. [S2] |
| Donor compensation ratio, η_n | 10 % | |
| Density of acceptors in the p-type region | 10^{18} cm^{-3} | |

| | | |
|--|---|---------------|
| Activation energy of acceptors | 0.37 eV | Ref. [S3] |
| Acceptor compensation ratio, η_p | 1 % | |
| Electron mobility in the n-type and p-type regions | 740 cm ² /Vs | Refs. [S1,S4] |
| Hole mobility in the n-type and p-type regions | 660 cm ² /Vs | Refs. [S1,S4] |
| Electron mobility in the i-type region | 2500 cm ² /Vs | Ref. [S5] |
| Hole mobility in the i-type region | 1200 cm ² /Vs | Ref. [S5] |
| Electron capture rate constant, c_n | $1.7 \times 10^{-8} \text{ cm}^3 \text{s}^{-1}$ | Ref. [S6] |
| Hole capture rate constant, c_p | $3.9 \times 10^{-7} \text{ cm}^3 \text{s}^{-1}$ | Ref. [S6] |
| Density-of-states effective mass for electrons | $1.64m_0$ | Ref. [S7] |
| Heavy-hole effective mass | $0.67m_0$ | Ref. [S7] |
| Light-hole effective mass | $0.26m_0$ | Ref. [S7] |
| Split-off effective mass | $0.38m_0$ | Ref. [S7] |

REFERENCES

[S1] R. S. Sussmann, *CVD Diamond for Electronic Devices and Sensors* (Wiley, New Jersey, 2009).

[S2] M. Katagiri, J. Isoya, S. Koizumi, and H. Kanda, Lightly phosphorus-doped homoepitaxial diamond films grown by chemical vapor deposition, [Appl. Phys. Lett. 85, 6365 \(2004\)](#).

[S3] M. Gabrysch, S. Majdi, A. Hallén, M. Linnarsson, A. Schöner, D. Twitchen, and J. Isberg, Compensation in boron-doped CVD diamond, [Phys. Status Solidi 205, 2190 \(2008\)](#).

[S4] J. Pernot, P. N. Volpe, F. Omnes, P. Muret, V. Mortet, K. Haenen, and T. Teraji, Direct measurement via cyclotron resonance of the carrier effective masses in pristine diamond, [Phys. Rev. B 81, 2967 \(2010\)](#).

[S5] C. E. Nebel, Electronic properties of CVD diamond, [Semicond. Sci. Technol. 18, S1 \(2003\)](#).

[S6] D. Yu. Fedyanin and M. Agio, Ultrabright single-photon source on diamond with electrical pumping at room and high temperatures, [New J. Phys. 18, 073012 \(2016\)](#).

[S7] N. Naka, K. Fukai, Y. Handa, and I. Akimoto, Direct measurement via cyclotron resonance of the carrier effective masses in pristine diamond, [Phys. Rev. B 88, 035205 \(2013\)](#).